

# Graph Recognition via Subgraph Prediction

André Eberhard<sup>1</sup>, Gerhard Neumann<sup>1</sup>, and Pascal Friederich<sup>1</sup>

<sup>1</sup> Karlsruhe Institute of Technology (KIT), Kaiserstraße 12, 76131 Karlsruhe, Germany  
 {andre.eberhard, gerhard.neumann, pascal.friederich}@kit.edu

**This work has been submitted to the IEEE for possible publication. Copyright may be transferred without notice, after which this version may no longer be accessible.**

**Abstract**—Despite tremendous improvements in tasks such as image classification, object detection, and segmentation, the recognition of visual relationships, commonly modeled as the extraction of a graph from an image, remains a challenging task. We believe that this mainly stems from the fact that there is no canonical way to approach the visual graph recognition task. Most existing solutions are specific to a problem and cannot be transferred between different contexts out-of-the box, even though the conceptual problem remains the same. With broad applicability and simplicity in mind, in this paper we develop a method, Graph Recognition via Subgraph Prediction (GraSP), for recognizing graphs in images. We show across several synthetic benchmarks and one real-world application that our method works with a set of diverse types of graphs and their drawings, and can be transferred between tasks without task-specific modifications, paving the way to a more unified framework for visual graph recognition.

## I. INTRODUCTION

One picture says more than a thousand words. Looking at pictures, humans can tell which entities are present and how they interact. Based on the identified entities and their relationships, we can understand complex scenes simply by looking at one frame. For computers, digital images are merely arrays of pixels, and their raw representation does not lend itself well to describe or understand the actual content of an image. Although the artificial intelligence community has made significant progress in identification [1], [2] and localization [3]–[5] of objects, the extraction of visual entities and their relationships remains a difficult problem. It has been formulated, among many distinct applications, as the extraction of a graph given an image, where the graph’s nodes describe the entities and edges their relationships. The applications range from early approaches of reversing graph drawings [6] to music recognition [7], medical image analysis [8], pose estimation [9], the recognition of road segments [10], molecules [11], [12] and scene graphs [13]–[19].

Conceptually, all these domains operate on a common ground: Given an image, the objective is to generate a graph representing the entities and relationships of interest. Technically, the solutions differ significantly from task to task and do not share any design principles, for which the reason is two-fold. First, different fields operate independently and propose independent solutions to domain-specific problems. Although all solutions aim to extract a graph from an image,

due to the generality and expressivity of graphs, the resulting techniques do not share many common traits, as the underlying problems themselves do not. Second, within the same task, especially if the task is new or difficult, many independent solutions are proposed for the same problem, each having its unique characteristics. We believe that this primarily stems from the fact that there is no canonical way to approach the image to graph translation conceptually, and each new method has to solve a common set of subproblems such as image processing, graph generation and optimization for the desired outcome. The major obstacle is how to model an expressive, discrete, compositional, and set-like structure with the currently available deep learning tools. Efforts to solve some of these subproblems are made within the field of *graph generative models* [20]–[22]. While they aim to model distributions of graphs, they do not have any connections to image processing.

To the best of our knowledge, there exists no general method for extracting graphs from images yet. Most works, such as those for recognizing molecules or scene graphs, either rely on complex pipelines involving multiple components or domain- or application-specific encodings [20], [23], which avoid working with an explicit graph representation altogether. The complexity and specificity of these methods limits their applicability and transferability to other contexts. As learned from the bitter lesson [24], methods built this way will not stand the test of time. Therefore, we believe that there should be a conceptual solution for recognizing graphs in images, rather than a collection of individual solutions to individual problems. This has the potential to unify many efforts across different tasks and domains by providing a unified framework. Ultimately, this will result in more general and powerful methods since efforts can be concentrated and improvements in one context may directly be transferred to others, as they share the underlying framework. In this paper, we present the first steps towards a more unified framework for visual graph recognition, termed **Graph Recognition via Subgraph Prediction**, or **GraSP**.

## II. GRAPHS AS MODEL OUTPUTS

Working with graphs as outputs of neural networks is not as straightforward as it is with other modalities such as images or text, primarily for two reasons.

**Graphs as compositional objects.** While images and text can be modeled as single units, graphs have a more compositional nature, which introduces additional challenges when using them as neural network outputs. When the task is, for example, to learn how to generate images, regardless of whether we use models such as Variational Autoencoders [25] or Diffusion Models [26], remarkable results can be achieved simply by applying some kind of pixel-wise loss, without taking the interaction of those pixels into account. In a similar vein, one can learn fascinating generative models of text by simply predicting which token would have appeared next in a large corpus of text, e.g., in GPT-style models [27], also not taking into account the interaction with other tokens for optimization. For graphs, this does not apply. When working with graphs as outputs of neural networks, we must make several predictions at once in order to arrive at a valid graph representation consisting of node and edge features as well as the edges themselves. This is further complicated by the edges being discrete and by variable-sized output graphs, i.e., graph sizes and connectivities. This introduces a source of methodological variability in the generation procedure, which we can highlight by looking at the methods proposed in the realm of graph generative modelling, a field also concerned with generating graphs but for modeling their distributions rather than image processing.

In [22], for example, the authors propose to generate a graph sequentially by introducing several stages of decision-making such as whether and where to add nodes and edges. Other methods, such as Graph Variational Autoencoders [28] or generative diffusion models for graphs [29], generate the output representation in one shot. Methods such as [21] propose to generate blocks of the adjacency matrix one block at a time, operating somewhere in between.

Both paradigms, sequential and one-shot generation, have their strengths and weaknesses. Sequential generation is flexible in how the graph is constructed and naturally handles variable-sized outputs and their orderings, but introduces additional latency during inference. One-shot generation is desirable in general as it is conceptually simpler and computationally more efficient, but does not address the way we represent graphs properly, a core problem that we further explain in the next paragraph.

**Graph isomorphism.** Regardless of the type of model we use, whether sequential, block-wise, or one-shot, once we have generated a graph with a randomly initialized model, we then must optimize the model’s parameters in order to produce meaningful graphs. For regression or classification tasks, optimization is well studied and standard. For graphs, this task becomes non-trivial for two reasons.

The first issue is caused by the fact that a graph’s representation is not unique and, due to graph isomorphism, an uncolored graph with  $n$  nodes has  $n!$  unique and equivalent representations. An ambiguous representation prevents us from applying unit losses used in regression and classification efficiently. When using one-shot methods that generate the whole structure at once then, implicitly, the model also encodes the ordering. In the realm of graph generative modelling, a common solution is to limit the number of potential orderings.

For example, fixed orderings such as BFS and DFS are common [20], [22]. Other methods, such as [30], try to match the ordering to produce a loss, making it part of the model implicitly. The authors in [21] even try to make the ordering adaptive.

The second issue is that due to the compositional nature of a graph, the outputs are not i.i.d. anymore, i.e., a suitable loss function would have to take into account the interplay between nodes, edges and potentially edge features. As a result, the optimization aspect when using graphs as model outputs becomes the major challenge, as it is unclear how to adjust the output towards the desired direction, especially as part of the output is discrete.

A core issue in many tasks where a graph is a neural network output is that it is difficult to build a decoder that receives an embedding in  $\mathbb{R}^d$  and implements an inverse mapping  $\mathbb{R}^d \mapsto \mathcal{G}$  where  $\mathcal{G}$  is the space of all graphs. We therefore believe that a more general method must be independent of the exact way we represent and generate the graph. The output representation being part of the model introduces a source of methodological variability as there are several ways to work around the aforementioned issues, and we believe that may be worthwhile to explore methods which do not explicitly rely on the output representation, thus avoiding these issues. Therefore, we argue that such a method should be built on top of a graph’s internal or conceptual representation rather than its output representation, which allows to treat graphs more like unit quantities and avoids issues related to how we need to represent a graph physically in a computer. Furthermore, we postulate that such a method must be sequential, as one-shot methods directly rely on the output representation and also introduce the aforementioned problems.

### III. PREDICTING SEQUENCES OF SUBGRAPHS

The vast majority of existing approaches using graphs of neural networks outputs first generates an output and applies some kind of loss to it, as is done with many other modalities. For graphs, unfortunately, supervision at the output introduces the aforementioned issues, which are hard to resolve in general. We instead propose to model the generation as a sequential decision-making procedure with step-wise supervision over subgraphs, which we formalize as a Markov Decision Process (MDP), defined by a set of states  $\mathcal{S}$ , actions  $\mathcal{A}$ , a transition function  $P$ , a reward function  $R$ , and no discount factor  $\gamma$ .

An intuitive approach for recognizing images in graphs by building them step-by-step would be as follows. Given an image  $\mathcal{I}$ , an initially random policy  $\pi$ , an initial graph  $\mathcal{G}_t$ , and a set of successor states  $\mathbb{G}_t = \{\mathcal{G}_{t+1} | P(\mathcal{G}_t, \mathcal{G}_{t+1}) > 0\}$ , we can produce sequences  $\mathcal{G}_t \dots \mathcal{G}_T$  where  $T$  corresponds to the last step in the sequence. Without loss of generality, we only consider transitions that add one edge at a time, either connecting a new node or two existing nodes. At every step, we choose  $\mathcal{G}_{t+1} = \arg \max_{\mathcal{G}_t \in \mathbb{G}_t} V^\pi(\mathcal{G}_t | \mathcal{I}) \forall t < T$ . Without making any other assumptions, the environment does not emit rewards for  $t < T$ , i.e., the reward is sparse. Upon completing the sequence with  $\mathcal{G}_T$  we can compare it to the graph  $\mathcal{G}_\mathcal{I}$

shown on the image, and receive a binary reward in  $\{0, 1\}$  indicating whether the generated graph is the correct one. We provide pseudocode Appendix D.

A common choice for optimization of  $\pi$  and/or  $V^\pi$  are reinforcement learning (RL) algorithms, such that the predictions favor states  $\mathcal{G}_t$  which are more likely to lead to the correct final prediction. While sound in theory, RL algorithms often have high data demands and show unstable training behavior. As in our scenario we are free to design the MDP, and hence know its dynamics, we do not need to apply RL and can improve the speed of learning by the following insight. We give an intuitive description of the complexity of learning an accurate value function interactively with RL for demonstrational purposes in Appendix E.

#### Replacing the value function with a binary classifier.

Given an infinite amount of time and under the assumption that rewards are only emitted upon termination and are in  $\{0, 1\}$ , the value function of the optimal policy,  $V^{\pi^*}$  would satisfy the following property: For any given graph  $\mathcal{G}_t$ ,  $V^{\pi^*}(\mathcal{G}_t | \mathcal{I}) = 1$  iff.  $\mathcal{G}_t \subseteq \mathcal{G}_{\mathcal{I}}$  and 0 otherwise. This stems from the fact that, whenever the sequence  $\mathcal{G}_t \dots \mathcal{G}_T$  terminates correctly, it must be a sequence of subgraphs of  $\mathcal{G}_{\mathcal{I}}$ . Whenever any  $\mathcal{G}_t$  is not a subgraph of  $\mathcal{G}_{\mathcal{I}}$ , it is impossible, without deletions, to arrive at  $\mathcal{G}_{\mathcal{I}}$ . This, in essence, allows us to forego learning the value function, and we can instead perform the task by learning a binary classifier, which we use in a sequential decoding procedure. From any  $\mathcal{G}_t$ , we can look at the possible set of modifications  $\mathbb{G}_t$ , and pick as  $\mathcal{G}_{t+1}$  any of the states which are a subgraph of the graph shown in the image, as predicted by the classifier. By adding to  $\mathbb{G}_t$  a self-transition indicating termination, we can iterate the procedure until the final result has been generated.

The prediction over full graphs has two important characteristics as a general method. First, explicit graph modification is not part of the model. This gives us flexibility in how we generate graphs and which graphs we present to the model. This makes the model agnostic of the type of graph it is working with. Second, step-wise predictions over full graphs do not have to deal with graph isomorphism and therefore do not need additional machinery for ordering and optimization. The prediction over full graphs subsumes all potential construction algorithms that incorporate more fine-grained decisions locally at each step. This makes the model agnostic of how the graph is built. By decoupling the model from both decision, i.e., what to add and where, and generation, i.e., in which order to do so, we can apply the same model to a large variety of graph recognition problems.

## IV. EFFICIENT TRAINING

We now proceed to describe how to efficiently train our model in practice. The three main components are data generation, neural network architecture and training. We describe our training architecture, configuration and hyperparameters in more detail in Appendix B.

**Data generation.** The first step in our setup is to generate data. The source of data can be arbitrary, either fully synthetic or based on existing datasets of graphs. One mild assumption

in our system is that it should be possible to sample a graph and draw it to obtain an image. In each iteration, we sample a target graph  $\mathcal{G}_T$  and retrieve some visual representation  $\mathcal{I}_{\mathcal{G}_T}$  of it. The next step is to generate triplets  $(\mathcal{I}_{\mathcal{G}_T}, \mathcal{G}_t, y)$  where  $\mathcal{G}_t$  is an arbitrary graph and  $y \in \{0, 1\}$  serves as the binary classification label depending on whether  $\mathcal{G}_t$  is a subgraph of  $\mathcal{G}_T$  or not. Without loss of generality, we generate positive samples  $\mathcal{G}_{T+}$  of subgraphs by deleting edges which do not disconnect the graph. We generate negative samples  $\mathcal{G}_{T-}$  by expanding the successor states  $\mathbb{G}_t$  and sampling a subset of these. While decomposed graphs are always subgraphs, for graphs in  $\mathbb{G}_t$  we run approximate subgraph matching to tell whether a sample is a subgraph or not. These algorithms are designed for matching graphs with hundreds or thousands of nodes, which is likely to suffice for most graphs in images. By sampling simulated transitions, we can guarantee that we cover the relevant subspace of graphs. While this is a sensible default, different kinds of graph recognition tasks may use any other sampling technique.

**Architecture.** The second step is to define an appropriate neural network architecture for the problem and learn its parameters. Formally, we learn a function  $f : (G, I) \mapsto \{0, 1\}$ , i.e., our setup is multi-modal, and we need to fuse visual and graph information. Since we learn over subgraphs, there are many graphs per image, which introduces redundancy of visual information that needs to be addressed. Instead of generating graph and image embeddings independently, we resort to FiLM-layers [31], where we use the graph embedding as a conditioner, and use the conditioned image embedding as input to a classification head. Figure 1 shows our simple feed-forward architecture schematically. Our Graph Neural Network (GNN) design follows the Message Passing Neural Network architecture [32], where we construct messages as the concatenation between source and target node features and the features of the edge connecting both nodes, as we generally train on graphs with both node and edge features. Our Convolutional Neural Network (CNN) design follows that of ResNet-v2 [33], where FiLM-layers are placed after every normalization layer within each block. The resulting output is a joint graph-image representation that can be used to predict whether this particular graph is a subgraph of the graph shown on the image. However, during decoding, the model needs to decide when to stop, which cannot be inferred from the embedding. As such, the model must distinguish between terminal and non-terminal subgraphs and must not yet stop when the current graph is not complete yet. To distinguish between both cases, we append a binary terminal flag to the graph-conditioned image embedding for prediction, and use it as input to the classification head. We provide more detailed description and justification of our architectural choices in Appendix C.

**Training.** To learn the binary classifier, what remains is to define an appropriate mini-batch sampling procedure which samples from the simulated transitions. Since the space of all image-graph pairs is large, we do not rely on a fixed pre-generated dataset and instead use a streaming architecture, where the aforementioned data generation procedure runs in parallel to training and provides the model with a continuous

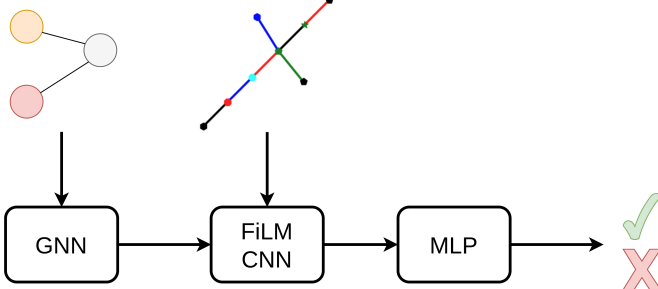


Fig. 1. Feed-forward architecture of our approach. The model first receives a graph as input and produces a graph embedding. This embedding is used to condition the image embedding on a particular graph. The prediction head uses this embedding, with an additional terminal flag, to predict whether a particular graph is a subgraph of the graph shown in the image.

stream of samples.

The data distribution based on our generation procedure has the following properties. We generate multiple image-graph pairs per image, which introduces data correlations between samples due to streaming data. We resolve these issues by maintaining two FIFO buffers for both positive and negative pairs, which in total hold  $B$  images and for each image we keep a small set of image-graph pairs. In addition, there are many more negative samples than positives, making the task highly imbalanced. To sample batches of diverse images, each entry in each buffer holds an image with their graphs and labels, and we always first sample an image and then a corresponding graph. To balance positive and negative samples, we sample half the batch size from each buffer in each step.

## V. RESULTS

In this section, we present our results in several synthetic benchmarks and one real-world scenario. To study the capabilities and limits of our proposed approach, we evaluate our method in a series of increasingly difficult tasks involving images of colored trees with a varying number of node and edge colors. In the synthetic benchmarks, we chose trees over graphs since they are planar and therefore clean to draw. Due to our streaming architecture, we do not have a natural definition of an epoch and measure all experiments by the number of samples processed. We evaluate 100 trajectories every 1M samples, i.e., one epoch corresponds to 1M samples. Every experiment has been conducted on 4 A100 GPUs with a time budget of 24h. Each trajectory starts with a randomly chosen node of the target graph and proceeds to expand and select successor graphs until a terminal action has been selected. A selection of a graph that is not a valid subgraph terminates the sequence immediately.

**Small colored trees.** In this section, we show our results on a synthetic benchmark dataset involving colored trees having six to nine nodes, where we vary the number of node and edge colors to vary task complexity. Figure 2a shows the accuracy of fully completed trajectories. As the results suggest, our model works well across multiple problem instances. Tasks involving only a small number of node and/or edge colors are solved quickly as there are fewer and easier decisions. For

harder tasks, the models take longer to converge. Figure 2b shows the trajectory length during evaluation over the course of training. Initially, the model selects many invalid successors which results in very short trajectories. Later in training, the model learns to generate longer valid sequences which directly correlates with the overall accuracy. Figure 2c shows the training loss, i.e., the cross-entropy for single transitions. The better the model predicts the sampled transitions, the higher the overall accuracy. Even though it looks like the loss is not decreasing in a meaningful way, the overall accuracy still increases due to small and important adjustments. We provide additional insights in Appendix F.

While standard evaluation metrics provide some insights about model performance, we can assess the expected performance of the model more reliably by evaluating its ability to avoid false positives, i.e., graphs not leading to the desired result. The metric we ultimately care about is the model's top- $k$  accuracy, i.e., whenever there are  $k$  valid choices, the model should not rank any false positives among its top- $k$  predictions. The top- $k$  accuracy to some degree measures the model's uncertainty between the positive and negative classes. A model that always assigns a very high probability to one of  $k$  positive choices and disregards the remainder could still achieve perfect accuracy in theory. In practice, however, it would be unreliable due to random fluctuations. Note that  $k$  is not fixed but varies depending on how many valid successor states there are. Figure 2d shows that our model consistently ranks positive samples above negatives.

While not a primary focus, we made one additional interesting observation during training. As we do not have a fixed dataset which we can split, in addition to in-distribution evaluation, i.e., graphs of size 6 to 9 encountered during training, we chose to evaluate on graphs of size 10 in order to guarantee that no such graph has been seen before. Figure 2e shows that our model also zero-shot generalizes to larger out-of-distribution (OOD) instances within the same problem class to some extent, which indicates that our multi-modal architecture is able to learn generalizable patterns independent of the actual size of the graph. Our model achieves this using only 7.25M parameters, which further highlights the benefits of our architecture.

The task involving only one node and edge color, even though the easiest in principle, stands out due to the behavior of message passing neural networks. When type information is absent, message passing becomes less informative as it is harder to break symmetries of similar neighbourhoods, which even causes the task to fail completely without taking this property of graph neural networks into account. To keep experiments consistent, we add learnable node degree embeddings to the input, which recovers the model's ability to break symmetries and to produce a meaningful graph embedding. This exemplifies the transferability of our approach between classes of tasks which only differ at the graph level but not otherwise. To apply our approach successfully to another class of problem one only needs to identify important properties of the current class of graphs, e.g., message passing pathologies in absence of type information, for which one can consult a large body of existing work in the mature field of graph

representation learning.

**Larger colored trees.** In the previous section, we conducted experiments on small instances of graphs. We further increase, using the same configuration, the sizes of graphs to range between 10 and 15 nodes. Figure 3a shows the overall accuracy over the course of training, which follow the same trend as on smaller instances, albeit slower due to increased computational demands and significantly harder task difficulty. Figure 3d shows the top-k accuracy. In contrast to the top-k accuracy on the smaller instances in Figure 2d, the model remains uncertain for an extended period but shows stable and consistent improvements during training. For evaluation, which include OOD graphs with 16 nodes, the trend also follows that the networks is able to extrapolate beyond graph sizes within the training distribution.

**Molecule recognition.** In this section, we evaluate our method on the challenging real-world application of Optical Chemical Structure Recognition (OCSR). OCSR tools aim to translate images of molecules into a machine-readable format. Before the advent of modern deep learning, rule-based systems such as OSRA [34] were dominant but are being replaced by modern deep learning alternatives due to their rigid nature of processing images. While rule-based OCSR systems are a class of tools on their own, deep learning tools can be split into two classes.

The first class treats OCSR as a graph recognition problem where the model output is a graph representing the molecule of interest. ChemGrapher [11] is a segmentation-based approach which uses crops of the final feature map as inputs to several classifiers for atoms and bonds and builds a graph based on the predictions. A more recent approach, MolGrapher [12], first outputs a set of key points, i.e., intersections of elements and bonds. It then constructs a super-graph from these elements, obtains embeddings via a graph neural network and then classifies the constituents. While these methods work well as a result of significant engineering efforts, they rely on pixel-level supervision as well as matching of the region to be classified to the corresponding label. Such approaches often have brittle hyperparameters such as crop-window sizes in ChemGrapher or bond lengths in MolGrapher, which may have major impacts on final performance. In MolGrapher, for example, the authors ablate one such parameter and find that setting it to a suboptimal value results in a drop of around ten percentage points. Breaking the end-to-end principle naturally lowers the upper bound of performance that can be achieved with such systems.

The second class of OCSR tools avoids these issues completely by framing it as a vision-language task. Tools such as DECIMER [23] use domain-specific encodings such as the Simplified Molecular Line Entry System (SMILES) [35] which encode the molecule as a string. Additionally, these strings can be canonicalized such that the order or elements becomes deterministic and allows for simple string comparison without the need to test for graph isomorphism. In turn, this allows to train sequence decoders from visual embeddings as deterministic tokens-level supervision becomes feasible. Without canonicalization, it would become significantly harder for a language model to represent the same entity with different

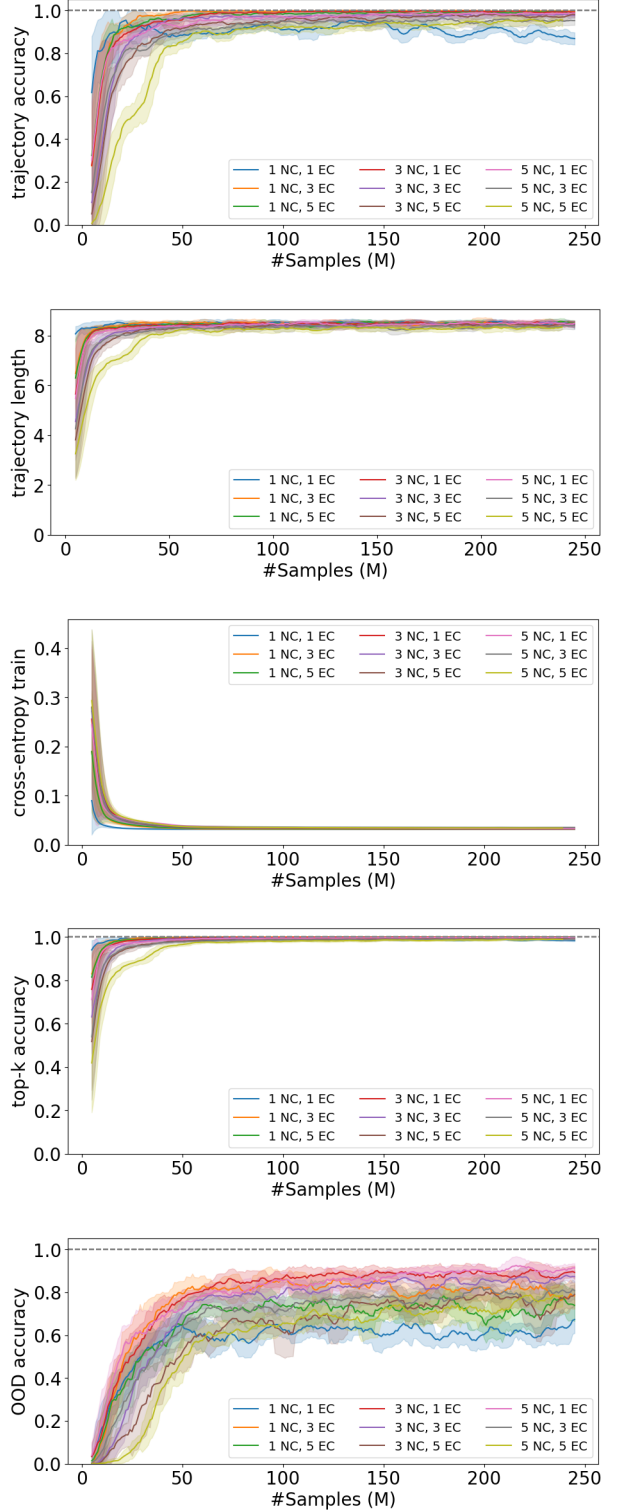


Fig. 2. Training dynamics of several synthetic tasks of varying complexity on trees with six to nine nodes. Shaded areas correspond to the standard deviation of a window of 10 iterations, i.e., 10M samples for training and 1000 trajectories for evaluation. Experiments X NC and Y EC have been conducted on graphs with X node and Y edge colors.  $k$  varies depending on the number of valid successor states.

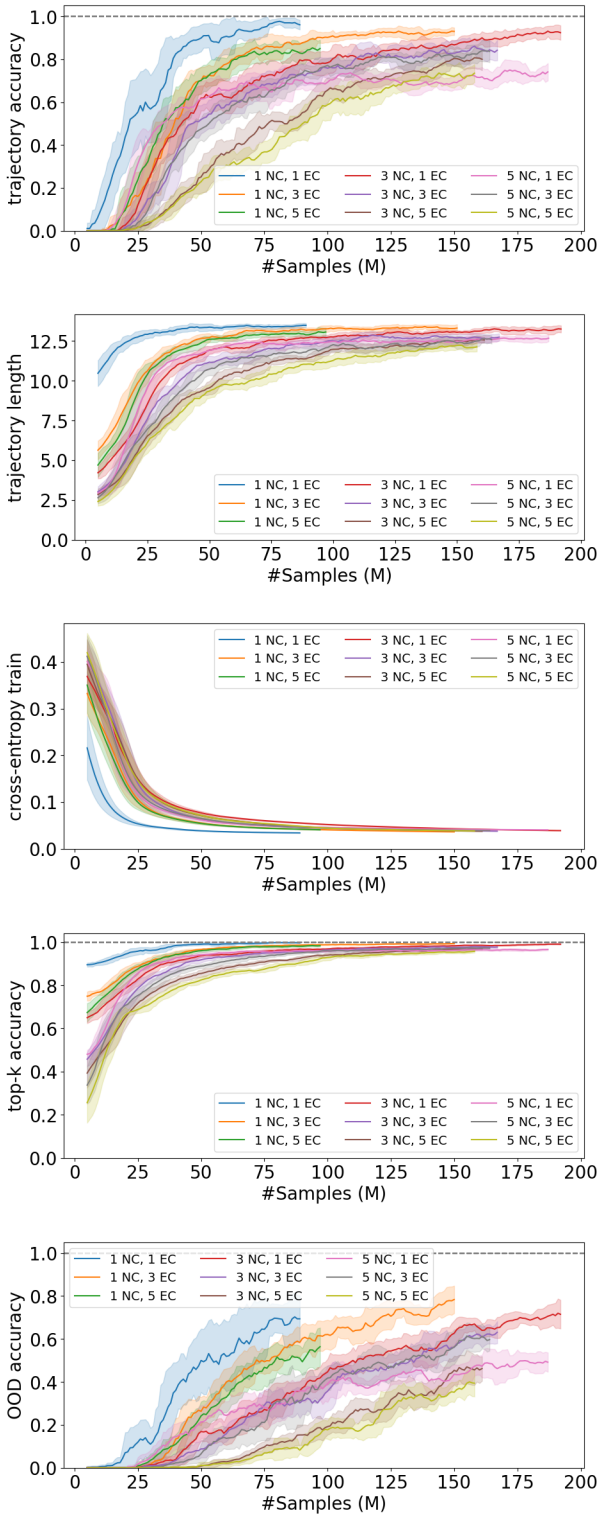


Fig. 3. Training dynamics of several synthetic tasks of varying complexity on trees with 10 to 15 nodes. Shaded areas correspond to the standard deviation of a window of 10 iterations, i.e., 10M samples for training and 1000 trajectories for evaluation. Experiments X NC and Y EC have been conducted on graphs with X node and Y edge colors.  $k$  varies depending on the number of valid successor states.

orderings.

In summary, at least for OCSR, existing solutions either rely on complex image processing, data labeling, and engineering or avoid working with graphs directly by reframing the problem. Neither methods which do not fully rely on learning nor those leveraging domain-specific information to circumvent issues unique to the problem will suffice to serve as generalizable approaches of the image-to-graph translation problem. In contrast, our proposed method possesses advantages of both approaches while lacking their disadvantages. *GraSP* outputs a proper graph representation while not building it from low-level pixel information and also does not rely on any domain-specific techniques to make the supervision more high-level, which highlights the advantages of our approach in practice.

For training and evaluation we use the QM9 [36] dataset. We randomly select a held-out test-set of 10,000 molecules and use the rest for training. Figure 4 shows, with the same evaluation procedure as for our synthetic tasks, the accuracy of our model over the course of training. Table I shows the performance of several OCSR tools on our held-out test set. While we do not match the performance of state-of-the-art tools, our model is still able to recognize a non-trivial fraction of test examples. Our main objective here is to highlight the transferability of our model and less its ability to achieve peak performance. In this context, we also would like to highlight the practical advantages of decoupling decision and generation, which may not be evident at first glance. When we transfer our model from colored trees to molecular graphs, the overall problem becomes slightly different. First, molecular graphs fall in the category of (mostly planar) graphs, and learning becomes slightly more challenging due to the increased structural complexity compared to trees. Second, the atom labels in molecular drawings carry semantic meaning, which the model needs to learn to distinguish. For example, long chains of carbon atoms are usually drawn as ragged lines, not carrying any visible atom label. Drawings frequently include groups like  $OH$  and  $NH$ , where the hydrogen atom is usually discarded in the molecular graph representation. Drawings also frequently include abbreviations of common functional groups consisting of multiple atoms. As decision is decoupled from generation, we are free to choose how to present such instances to our model. In practice this means that we can choose from the full spectrum of granularity. On one hand, we can choose to represent a functional group as one distinct type, which increases the breath and reduces the depth of trajectories. On the other hand, we can choose to not explicitly include a functional group as decision but rather work on an expanded graph, which increases the depth but reduces the breath of trajectories. This highlights that the ability to incorporate domain knowledge arises by design, as we are free to define the state space and transition dynamics in our MDP.

For demonstrational purposes, in our OCSR benchmark, we can apply rules such as not to extend the current graph further at nodes which have a node degree of four due to the rules of chemistry, which helps the model to focus its capacity on a more relevant subspace. We keep this modification purely at a graph level and do not further incorporate more fine-grained

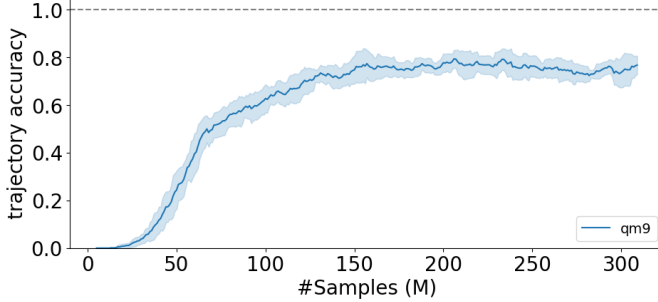


Fig. 4. Accuracy on the QM9 dataset.

chemistry rules.

	OSRA	GraSP (ours)	MolGrapher	DECIMER
Accuracy	45.61%	67.51%	88.36%	92.08%

TABLE I

ACCURACY ON QM9 IMAGES WITH NO STEREO-BONDS AND IN GRayscale. WE RANDOMLY SELECT 10,000 IMAGES FOR EVALUATION AND KEEP THE REST FOR TRAINING.

## VI. DISCUSSION

In this paper, we presented a general framework, *GraSP*, for graph recognition in images. By addressing common issues of using graphs as neural network outputs, we derived a generic, efficient and flexible formulation of sequential graph generation conditioned on an image. We demonstrated the capabilities of our model on several graph recognition tasks of varying complexity, where we show that *GraSP* allows for seamless transfer between different tasks, leaving open the possibility to leverage domain-specific information. In general, training models under our framework is stable and yields models that generalize well both on in- and out-of-distribution data. Our approach of sampling simulated transitions naturally scales to distributed training architectures, and allows for practical training on large and complex graph datasets and with large neural networks, whenever scale is required. To conclude, we would like to highlight several implications of our design principles and also highlight which issues need to be addressed in future extensions of the framework.

First, we assume a finite set of types for both nodes and edges. While many tasks fall under this category, other real-world tasks may include categories more loosely. An interesting avenue to explore would be to use text embeddings of large language models to model categories and their interactions, thus extending the framework with an open vocabulary component, which would make our framework applicable to much more challenging tasks such as scene graph recognition.

Second, for very large graphs, we need to balance the breadth and depth of trajectories for efficient inference. The model quickly learns that the majority of states are easy negative samples, and only a few states effectively are considered for decoding. This indicates that it may be beneficial to first rule out irrelevant states by a learned filter on possible relations. For example, in a large colored graph, whenever we exhausted a particular relation, e.g., two red nodes connected

by a black edge, we need not consider it in subsequent steps, which may reduce the branching factor considerably. In our current setup, the set of successor states includes these relations even though they are irrelevant. It is the decoding component that truly prevents us from applying our model to much larger graphs efficiently. In contrast, our learning component mostly relies on graph embeddings and will further benefit from future developments in graph representation learning.

Third, while we primarily focused images as input modality, another interesting avenue would be to combine our decoding procedure with other modalities, specifically vector embeddings of graphs.

## REFERENCES

- [1] A. Krizhevsky, I. Sutskever, and G. E. Hinton, “Imagenet classification with deep convolutional neural networks,” *Advances in neural information processing systems*, vol. 25, 2012.
- [2] K. He, X. Zhang, S. Ren, and J. Sun, “Deep residual learning for image recognition,” in *Proceedings of the IEEE conference on computer vision and pattern recognition*, 2016, pp. 770–778.
- [3] R. Girshick, J. Donahue, T. Darrell, and J. Malik, “Rich feature hierarchies for accurate object detection and semantic segmentation,” in *Proceedings of the IEEE conference on computer vision and pattern recognition*, 2014, pp. 580–587.
- [4] O. Ronneberger, P. Fischer, and T. Brox, “U-net: Convolutional networks for biomedical image segmentation.” Springer, 2015, pp. 234–241.
- [5] J. Redmon, S. Divvala, R. Girshick, and A. Farhadi, “You only look once: Unified, real-time object detection,” in *Proceedings of the IEEE conference on computer vision and pattern recognition*, 2016, pp. 779–788.
- [6] C. Auer, C. Bachmaier, F. J. Brandenburg, A. Gleißner, and J. Reislhuber, “Optical graph recognition,” in *Graph Drawing: 20th International Symposium, GD 2012, Redmond, WA, USA, September 19-21, 2012, Revised Selected Papers 20*. Springer, 2013, pp. 529–540.
- [7] C. Garrido-Munoz, A. Rios-Vila, and J. Calvo-Zaragoza, “A holistic approach for image-to-graph: application to optical music recognition,” *International Journal on Document Analysis and Recognition (IJDAR)*, vol. 25, no. 4, pp. 293–303, 2022.
- [8] D. Ahmed-Aristizabal, M. A. Armin, S. Denman, C. Fookes, and L. Petersson, “Graph-based deep learning for medical diagnosis and analysis: past, present and future,” *Sensors*, vol. 21, no. 14, p. 4758, 2021.
- [9] Z. Cao, T. Simon, S.-E. Wei, and Y. Sheikh, “Realtime multi-person 2d pose estimation using part affinity fields,” in *Proceedings of the IEEE conference on computer vision and pattern recognition*, 2017, pp. 7291–7299.
- [10] D. Belli and T. Kipf, “Image-conditioned graph generation for road network extraction,” *arXiv preprint arXiv:1910.14388*, 2019.
- [11] M. Oldenhof, A. Arany, Y. Moreau, and J. Simm, “Chemgrapher: optical graph recognition of chemical compounds by deep learning,” *Journal of chemical information and modeling*, vol. 60, no. 10, pp. 4506–4517, 2020.
- [12] L. Morin, M. Danelljan, M. I. Agea, A. Nassar, V. Weber, I. Meijer, P. Staar, and F. Yu, “Molgrapher: Graph-based visual recognition of chemical structures,” in *Proceedings of the IEEE/CVF International Conference on Computer Vision (ICCV)*, 10 2023, pp. 19 552–19 561.
- [13] Y. Zhao and S.-C. Zhu, “Scene parsing by integrating function, geometry and appearance models,” in *Proceedings of the IEEE conference on computer vision and pattern recognition*, 2013, pp. 3119–3126.
- [14] C. Lu, R. Krishna, M. Bernstein, and L. Fei-Fei, “Visual relationship detection with language priors,” in *Computer Vision–ECCV 2016: 14th European Conference, Amsterdam, The Netherlands, October 11–14, 2016, Proceedings, Part I 14*. Springer, 2016, pp. 852–869.
- [15] K. Tang, Y. Niu, J. Huang, J. Shi, and H. Zhang, “Unbiased scene graph generation from biased training,” in *Proceedings of the IEEE/CVF conference on computer vision and pattern recognition*, 2020, pp. 3716–3725.
- [16] J. Yang, J. Lu, S. Lee, D. Batra, and D. Parikh, “Graph r-cnn for scene graph generation,” in *Proceedings of the European conference on computer vision (ECCV)*, 2018, pp. 670–685.

- [17] R. Yu, A. Li, V. I. Morariu, and L. S. Davis, “Visual relationship detection with internal and external linguistic knowledge distillation,” in *Proceedings of the IEEE international conference on computer vision*, 2017, pp. 1974–1982.
- [18] G. Chen, J. Li, and W. Wang, “Scene graph generation with role-playing large language models,” *Advances in Neural Information Processing Systems*, vol. 37, pp. 132 238–132 266, 2024.
- [19] J. Im, J. Nam, N. Park, H. Lee, and S. Park, “Egrt: Extracting graph from transformer for scene graph generation,” in *Proceedings of the IEEE/CVF conference on computer vision and pattern recognition*, 2024, pp. 24 229–24 238.
- [20] J. You, R. Ying, X. Ren, W. Hamilton, and J. Leskovec, “Graphrn: Generating realistic graphs with deep auto-regressive models,” in *International conference on machine learning*. PMLR, 2018, pp. 5708–5717.
- [21] R. Liao, Y. Li, Y. Song, S. Wang, W. Hamilton, D. K. Duvenaud, R. Urtsasun, and R. Zemel, “Efficient graph generation with graph recurrent attention networks,” *Advances in neural information processing systems*, vol. 32, 2019.
- [22] Y. Li, O. Vinyals, C. Dyer, R. Pascanu, and P. Battaglia, “Learning deep generative models of graphs,” *arXiv preprint arXiv:1803.03324*, 2018.
- [23] K. Rajan, H. O. Brinkhaus, M. I. Agea, A. Zielesny, and C. Steinbeck, “Decimer. ai: an open platform for automated optical chemical structure identification, segmentation and recognition in scientific publications,” *Nature communications*, vol. 14, no. 1, p. 5045, 2023.
- [24] R. Sutton, “The bitter lesson,” *Incomplete Ideas (blog)*, vol. 13, no. 1, p. 38, 2019.
- [25] D. P. Kingma and M. Welling, “Auto-encoding variational bayes,” in *2nd International Conference on Learning Representations, ICLR 2014, Banff, AB, Canada, April 14-16, 2014, Conference Track Proceedings*, Y. Bengio and Y. LeCun, Eds., 2014. [Online]. Available: <http://arxiv.org/abs/1312.6114>
- [26] J. Ho, A. Jain, and P. Abbeel, “Denoising diffusion probabilistic models,” *Advances in neural information processing systems*, vol. 33, pp. 6840–6851, 2020.
- [27] T. Brown, B. Mann, N. Ryder, M. Subbiah, J. D. Kaplan, P. Dhariwal, A. Neelakantan, P. Shyam, G. Sastry, A. Askell *et al.*, “Language models are few-shot learners,” *Advances in neural information processing systems*, vol. 33, pp. 1877–1901, 2020.
- [28] T. N. Kipf and M. Welling, “Variational graph auto-encoders,” *arXiv preprint arXiv:1611.07308*, 2016.
- [29] J. Jo, S. Lee, and S. J. Hwang, “Score-based generative modeling of graphs via the system of stochastic differential equations,” in *International conference on machine learning*. PMLR, 2022, pp. 10 362–10 383.
- [30] M. Simonovsky and N. Komodakis, “Graphvae: Towards generation of small graphs using variational autoencoders,” in *International conference on artificial neural networks*. Springer, 2018, pp. 412–422.
- [31] E. Perez, F. Strub, H. De Vries, V. Dumoulin, and A. Courville, “Film: Visual reasoning with a general conditioning layer,” in *Proceedings of the AAAI conference on artificial intelligence*, vol. 32, no. 1, 2018.
- [32] J. Gilmer, S. S. Schoenholz, P. F. Riley, O. Vinyals, and G. E. Dahl, “Neural message passing for quantum chemistry,” in *International conference on machine learning*. PMLR, 2017, pp. 1263–1272.
- [33] K. He, X. Zhang, S. Ren, and J. Sun, “Identity mappings in deep residual networks,” in *Computer Vision–ECCV 2016: 14th European Conference, Amsterdam, The Netherlands, October 11–14, 2016, Proceedings, Part IV 14*. Springer, 2016, pp. 630–645.
- [34] I. V. Filippov and M. C. Nicklaus, “Optical structure recognition software to recover chemical information: Osra, an open source solution,” 2009.
- [35] D. Weininger, “Smiles, a chemical language and information system. 1. introduction to methodology and encoding rules,” *Journal of chemical information and computer sciences*, vol. 28, no. 1, pp. 31–36, 1988.
- [36] R. Ramakrishnan, P. O. Dral, M. Rupp, and O. A. Von Lilienfeld, “Quantum chemistry structures and properties of 134 kilo molecules,” *Scientific data*, vol. 1, no. 1, pp. 1–7, 2014.
- [37] T.-Y. Lin, P. Goyal, R. Girshick, K. He, and P. Dollár, “Focal loss for dense object detection,” in *Proceedings of the IEEE international conference on computer vision*, 2017, pp. 2980–2988.
- [38] T. Ridnik, E. Ben-Baruch, N. Zamir, A. Noy, I. Friedman, M. Protter, and L. Zelnik-Manor, “Asymmetric loss for multi-label classification,” in *Proceedings of the IEEE/CVF international conference on computer vision*, 2021, pp. 82–91.
- [39] L. Liu, H. Jiang, P. He, W. Chen, X. Liu, J. Gao, and J. Han, “On the variance of the adaptive learning rate and beyond,” *arXiv preprint arXiv:1908.03265*, 2019.

## APPENDIX A ONLINE REPOSITORY

We provide additional information in an anonymized GitHub repository located at: <https://github.com/c72bcbf4/grasp>. Reviewers are encouraged to try out our model interactively and see how

## APPENDIX B EXPERIMENTAL SETUP

**Data Generation.** *GrASP*, as a theoretical framework, only prescribes that we can extract graphs from images by search for subgraphs. In practice, we need to instantiate a dataset to train the model. We chose the following sequence of steps for sample creation. References to code can be found in the README of the project. All parameters are summarized in Table II.

- 1) We sample a target graph and generate a corresponding image of it.
- 2) We then need to decide how and how many subgraphs with labels to generate per image, since we need both diverse images and image-graph pairs. To obtain image-graph pairs, we run several DFS decompositions of the target graph by deleting edges that do not disconnect the graph. To avoid duplicates, we hash every graph and skip decomposition branches which were visited before. This yields a set of positive training examples, as all decomposed graphs are trivially subgraphs of the target graph.
- 3) We then need to proceed to generate negative examples, which we do, for every positive subgraph in the previous step, by looking at a subset of possible modifications and the resulting graphs. By approximate graph matching, we decide whether a successor is a positive or negative instance, and add these samples to our dataset.
- 4) As our algorithm must distinguish between terminal and non-terminal graphs, we add to each graph a terminal self-transition, which we use during decoding. A terminal subgraph is only a positive instance if it is the target graph and not otherwise.

As we are free to choose the data distribution, we randomly select 10% of all samples to be terminal states. To limit the number of graphs per image, from all successors, we sample only 5 successors corresponding to node and 5 successors corresponding to edge additions.

**Mini-batch selection.** The above procedure generates a stream of correlated image-graph pairs, violating the i.i.d. assumption. Furthermore, this stream contains more positive than negative samples, which makes the classification task imbalanced. While techniques like re-weighting losses based on class imbalance or self-balancing losses like Focal Loss [37] and Asymmetric Loss [38] were designed to address such issues, they introduce hard-to-tune hyperparameters, which we were unable to use without destabilizing training. We therefore decided to balance mini-batches at the data-level by introducing two temporary buffers instead of one, each keeping positive and negative samples, respectively.

**Training.** We measure training process as the number of samples processed since we do not have the definition of an epoch due to our streaming architecture. We evaluate 100 trajectories after each  $1M$  processed samples. Training is conducted on a machine with 4 A100 GPUs and 48 cores. We train with both learning rate warmup and decay with a mini-batch size of 1024. We apply gradient clipping to prevent excessive updates. To stabilize training especially early in training until a sufficient number of diverse samples has been generated, we use the RAdam [39] optimizer with no weight decay.

Parameter	Value
fraction of terminal samples	0.1
decompositions per graph	10
max. node additions per subgraph	5
max. edge additions per subgraph	5
label smoothing	0.01
samples per evaluation	$1M$
trajectories per evaluation	100
mini-batch size	1024
max. gradient norm	1.0
weight decay	0.0
dropout	0.0
learning rate	$5 \times 10^{-4}$ cosine schedule, start and end $5 \times 10^{-4}$ , warmup 50M samples, cycle 250M samples
learning rate schedule	
buffer size	25,000 images

TABLE II  
HYPERPARAMETERS FOR ALL RUNS.

## APPENDIX C ARCHITECTURE

In this section, we discuss the rationale behind our architectural choices in much greater detail.

**FiLM layer usage.** Our setup is multi-modal and an appropriate architecture must properly account for this. A first question that may arise is why we condition image embeddings on the graph embedding and not vice versa. Our framework does not prescribe any particular neural network architecture. We believe that our choice is slightly more flexible. One reason is that CNNs are rather rigid compared to GNNs and there are fewer choices in general where to place the conditioning within a convolutional block, which is a minor implementational detail. The more important reason of generating the graph embedding first for conditioning is that for transfer between tasks, it may be necessary to switch to a more appropriate GNN for a particular task, whereas a CNN is powerful enough to extract general patterns from a much wider range of images and may need only simple adjustments in width and depth, depending on the properties of the image. Therefore, it is much easier to experiment with different graph neural network architectures. Otherwise, for each new architecture, one must implement a FiLM-compatible version of every popular variant.

**Normalization layers.** In our setup, which is distributed by default, one must choose appropriate normalization layers.

In general, we avoid Batch Normalization in all modules, as it must be synchronized between devices. For the CNN, we therefore settled for Group Normalization as a compromise between Layer Normalization and Instance Normalization. We use 8 groups independent of the number of channels in each layer, i.e., more filters in a convolutional layer result in larger but not more groups. For the GNN, Instance Normalization and Graph Normalization seem like strong contenders at first sight, as they normalize over the full graph, whereas Batch Normalization would normalize over a batch of graph with a variable number of nodes which results in inaccurate statistics and is susceptible to leakage effects between graphs. However, as we work with a wide range of graph sizes, including pathological examples like single-node graphs, we find Layer Normalization more robust as we do not need to account for such effects. For the MLP, we also use Layer Normalization.

**Termination flag.** During decoding, which is explained in detail in Appendix D, we need to be able to decide when to terminate. As we cannot infer this from the graph only, we need an additional termination flag as input. We append the terminal indicator to the graph-conditioned image embedding and not to the graph for the following reason. In case we append an additional dimension to the graph embedding, we essentially create two graph separate graph spaces for conditioning instead of a shared one, which is not what we want. Therefore, the terminal flag is used as an input to the classification head, which can then learn to separate the terminal from the non-terminal space. This keeps learning of the joint representation slightly more efficient as the network does not need to learn to distinguish between terminal and non-terminal states at this stage of the forward pass.

#### APPENDIX D PSEUDOCODE

##### Algorithm 1 Graph Recognition via Subgraph Prediction

---

```

1: Input: image  $\mathcal{I}$ , modification set  $\mathbb{M}$ , policy  $\pi$ 
2:  $\mathcal{G}_t \leftarrow \emptyset$ 
3: while not done do
4:    $\mathbb{G}_t \leftarrow \{ \text{expand}(\mathcal{G}_t, m) \mid m \in \mathbb{M} \}$ 
5:    $\mathcal{G}_{t+1} = \arg \max_{\mathcal{G}_t \in \mathbb{G}_t} V^\pi(\mathcal{G}_t | \mathcal{I})$ 
6:    $\mathcal{G}_t \leftarrow \mathcal{G}_{t+1}$ 
7: end while
8: Return:  $\mathcal{G}_t$ 

```

---

In *GraSP*, inference is a simple recursive procedure. We start with an empty graph and add to it all possible modifications, yielding the set of successor states  $\mathbb{G}_t$ . We collate this into a batch of examples and run a forward pass. As we only need to decide whether or a sample is valid, i.e., whether it corresponds to the positive class, we simply can use a greedy decoding procedure since an accurate model should always rank positive examples above negatives.

#### APPENDIX E COMPLEXITY OF THE STATE SPACE

We briefly want to highlight the computational complexity of the search space of our proposed approach and the effi-

ciency gains of our formulation of the problem. Assuming we only add one node or edge at a time, the number of valid intermediate steps directly corresponds to the number of connected subgraphs of a graph, for which we can distinguish between three classes of graphs. In general as there are up to  $2^n$  induced subgraphs for a graph with  $n$  nodes and the exact number depends on the topological properties of a graph. First, for trees, the number of subgraphs grows polynomially in  $n$ . Second, for general graphs, the number grows exponentially in  $n$ . And third, for planar graphs, the number is larger than for trees but smaller on average than for non-planar graphs. Therefore, learning an accurate value function includes the exploration and evaluation of exponentially many states for just one example, not taking into account the number of steps that result in exploration of the space of non-subgraphs. Generalization over a relevant subspace therefore requires a considerable amount of computation for interaction and value function learning without ground-truth values.

#### APPENDIX F OPTIMIZATION DYNAMICS

In this section we give some insights about the optimization dynamics during training. The results in the main section indicate that the method quickly and stably reaches a good level of performance. After this point, the model seems to learn only slowly, as can be measured by the loss (5a), gradient norms (5b) and accuracy (5d). However, when looking at the output logits (5a), we can see that the model keeps learning, although slowly. While initially biased towards negative outputs, over the course of training the model recovers more balanced outputs, which we found is usually the case for well-performing and converged models. For our larger experiments in Figure 6, this behavior is analogous and the models simply need more time to converge.

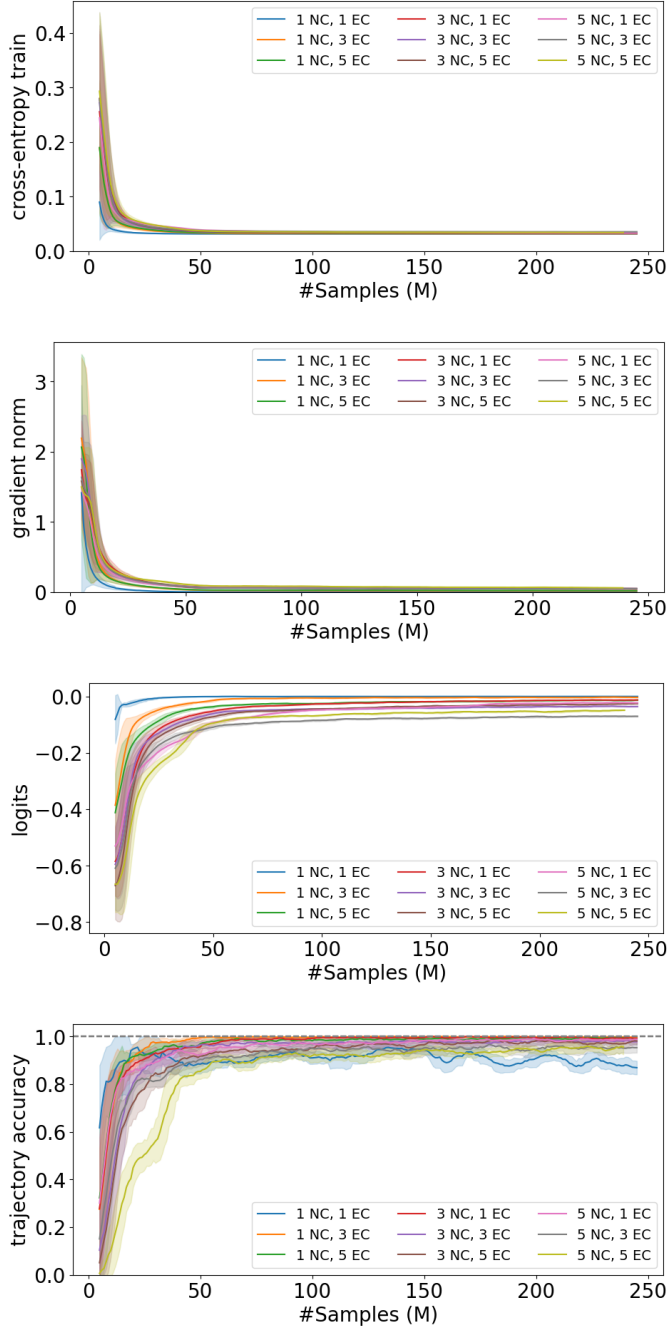


Fig. 5. Training dynamics for graphs of size 6 to 9.

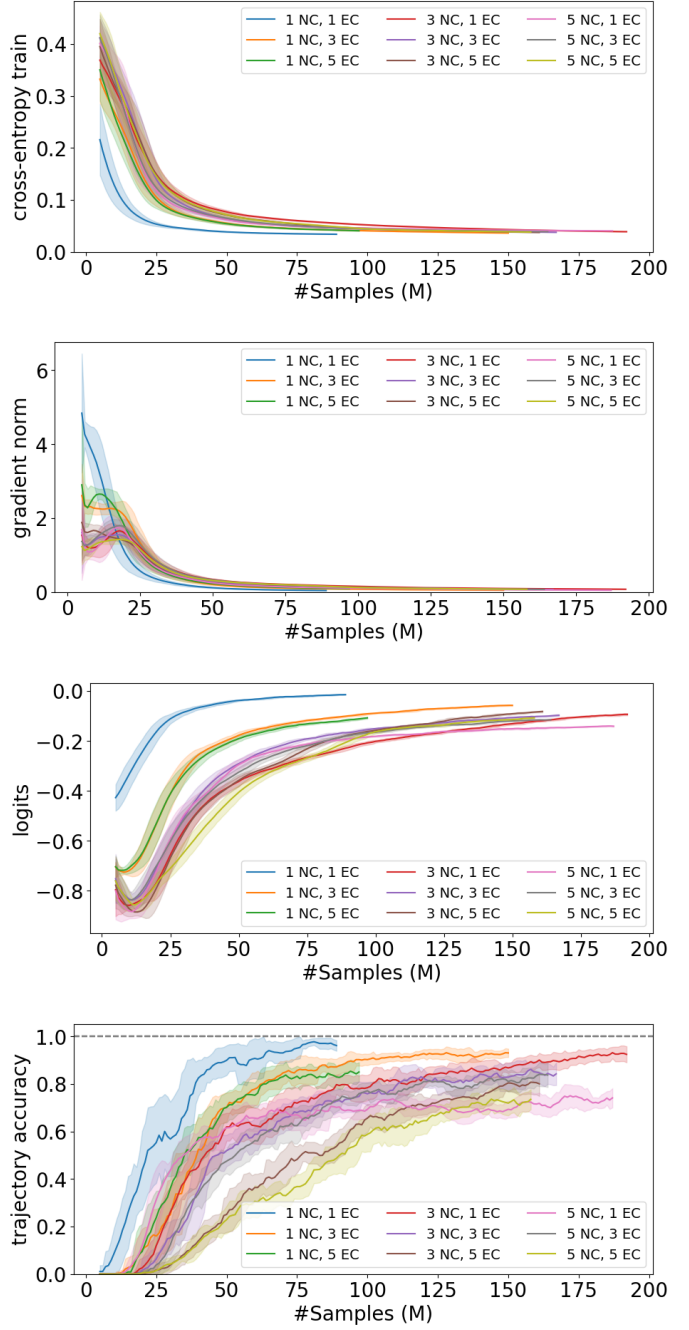


Fig. 6. Training dynamics for graphs of size 10 to 15.